Using LiDAR DTMs data for river sediment transport

HSIEH Yuchung[1, 3], CHAN Yuchang[2], HU Jyrching[1], LIN Chaochung[3]

1. *Department of Geosciences, Taiwan University, Taiwan 10617, China*;
2. *Institute of Earth Sciences, Taiwan 11581, China*;
3. *Central Geological Survey, Taiwan 23585, China*

Abstract: Taiwan is located in a subtropical region and issusceptible to typhoons and torrential rains during the summer seasons. Taiwan is also located on actively shifting tectonic plates that can cause dramatic terrain changes. Taiwan's river terrain frequently sustains substantial changes, especially after typhoons and torrential rains. Presently, digital terrain maps or models made by airborne LiDAR technology are reliable, have sufficient resolutions, are accurate, convenient, and can filter out buildings or tree cover to restore the original ground topography. This type of map or model can meet the requirements of geological and topographical analysis studies. In 2008, the Lanyang River region experienced four major typhoon events: Kalmaegi, Fung-Wong, Sinlaku, and Jangmi. These typhoons changed the riverbed terrain dramatically. Therefore, we used two occasions of digital terrain data measured using the airborne LiDAR system to conduct analytical comparisons of the riverbed terrain and river sediment transportation changes before and after typhoon events. The study is the first of its kind to demonstrate the excellent applications of the airborne LiDAR system for measuring river terrains in a large watershed area; digital terrain data were produced for periods before and after a typhoon season. We used the elevation difference topography measurement method to calculate river terrain changes before and after a typhoon season. This study's results showed that the airborne LiDAR high resolution digital terrain model data produced excellent results when used to calculate river terrain and sediment volume changes or change amounts.

Key words: Lanyang river, typhoon torrential rain events, geomorphological features, airborne LiDAR, digital terrain model

CLC number: TP95 **Document code:** A

Citation format: **Hsieh Y C, Chan Y C, Hu J C, Lin C C. 2013. Using LiDAR DTMs data for river sediment transport. Journal of Remote Sensing, 17(1): 193–209**

1 INTRODUCTION

Taiwan is located in a subtropical region and is susceptible to typhoons and torrential rains during the summer. Taiwan is also located in an area of active tectonic plate movements and experiences continuous activity of geological structure that cause dramatic terrain alterations. Especially after typhoons and torrential rain, river terrains generate tremendous changes. The Lanyang River is one of the major rivers in Taiwan. It is often directly affected by typhoons and torrential rains originating from the Pacific Ocean in the summer. The natural erosions and collapses upstream cause generated sediments to follow runoff and be transported to the downstream river area. This causes high riverbed silt, scour effect, or changes to the river channel in the mid to downstream areas. The unit annual sediment runoff or transported sediment volume of Taiwan's major rivers is more than 6000 t/km^2 kilometer. The annual sediment yield of the Lanyang Riverexceeds 40,000 t/km^2. Furthermore, statistical research related to riverbed terrain changes and sediment runoff or transportation volume is a critical topic for soil and water conservation, water conservancy planning, and river ecological habitat changes.

The Digital Elevation Model (DEM) provides excellent application in the geology and geomorphology fields. The DEM can present flat or three-dimensional models when needed and can effectively illustrate topographical features from various angels. The Digital Terrain Model (DTM) acquisition methods include terrain contour lines, side-looking radar, satellite images, aerial photos, the Real Time Kinematic Global Positioning System (rtkGPS), total station theodolite (total stations), and LiDAR systems (airborne andterrestrial LiDAR). As the technology for terrain measurement advances, terrain data accuracy and resolution has improved. Various terrain measurement methods and achievements have employed enhancements in terrain data to present improved results. Previously regarding river terrain research, digital terrain data were mainly used in river geomorphology, river cross-sectioning, and longitudinal profile or section change-related analysis (Lane, 1998). Since the 1990s, digital terrain model data collected by overlapping terrain surveys from different periods have been used to construct river topography of various periods.

Received: 2012-01-15; **Accepted:** 2012-08-24

First author biography: HSIEH Yuchung (1974—), male , Ph.D. candidate .His research interests are geological survey and remote sensing application about geological hazard. E-mail:spencer1121@gmail.com

Corresponding author biography: CHAN Yuchang (1966—), male, professor. His research interests are structure geology, geotectonic and remote sensing geology. E-mail: yuchang@earth.sinica.edu.tw

The elevation difference values from terrain changes during different periods have been used to develop various river topography measurements (Lane, et al., 1994; Brasington, et al., 2003; Lane, 1998; Lane, et al., 2003; Milan, et al., 2007; Rumsby, et al., 2008; Wheaton, et al., 2009). River terrain change elevation difference values can be used to understand the local extent of river accumulation and erosion, project actual accumulation and erosion volume changes for the river channel, and form an integrated projection of the total volume changes for river terrain changes. The majority of the studies discussed above used the digital terrain model data produced through aerial surveys and rtkGPS technologies for calculations. In addition to limiting the scope of research to a range of several square kilometers, the error differences from differing technologies increases the complex variables for terrain change calculations. Using airborne LiDAR system technology from different periods can be applied to monitor and analyze larger river basins and watersheds or landslide areas (Cavalli, et al., 2008). Studies conducted in Taiwan also used digital terrain models produced by aerial photos before and after typhoon disasters to analyze and calculatethe DTM differences for before and after typhoons and calculate or project possible sediment yield volume (Zheng, et al., 2005), and have also used SPOT imaging and DTM to estimate sediment yield volume (Jiang, et al., 2007).

In June 2008, after the LiDAR digital terrain measurement of the mid- and upstream portions of the Lanyang River was completed, the Lanyang River experienced four severe typhoons: Kalmaegi, Fung-Wong, Sinlaku, and Jangmi. These typhoons caused dramatic changes to the riverbed terrain. Therefore, we conducted airborne LiDAR terrain measurement a second time in October 2008 for an identical river channel range of approximately one hundred square kilometers. We used the airbone LiDAR system for the first time to measure the river terrain of a large watershed area. Digital terrain data were produced for different periods before and after the typhoon season. The elevation difference value topography measurement method was employed to calculate the terrain changes of the Lanyang River before and after typhoon season and analyze and compare riverbed topography and river sediment transport changes before and after the typhoon incidents.

2 STUDY AREA

We selected the mid- and upstream region of the Lanyang River as the survey site for this study. The Lanyang River was originally named the Zhuoshui River of Yilan County, and obtained its namefor its rich sediment content and water turbidity. It is one of the major rivers in Taiwan and the largest riverin northeastern Yilan County, and originates from the northern Nanhu mountain foothills. From its origination point, the Lanyang River zigzags between the Snow Mountain Range and the Nanhu Mountain Range and flows northeast to Phoa-po-o, where it begins to enter the flat lands. The stream bifurcates or forms branches into reticular turbulences, developing a main stream near the Lanyang Bridge, and finally flows east into the Pacific Ocean. Its watershed or river basin area is approximately 978 km^2, and the length of the mainstream is approximately 73 km.

The mainstream of the Lanyang River is a torrent-river. The steep slopes and rapid currents upstream frequently discharge large amounts of sediment during flood periods. During concentrated rainfall, large flood water flow can produce severe damaging impacts. Over the years, the straight or direct impact of the mainstream flood flowhas caused disasters and scoured the feet of embankments and damaged embankment slopes with flood debris abrasion.

The location of the study area was the mid- and upstream Lanyang River watershed area near the Yingshi and Siji villages (Fig.1). It is located between Taiwan’s northeastern Central Mountain Range and the Snow Mountain Range regions. From remote sensing images, the main Lanyang River channel forms an obvious linear shape. This line begins at Niutou and extends south-southwest toward the upper reaches of the Lanyang River. Many geologists have referred to this line as the Lishan fault (Ho, 1975; Wu, 1976) or the Niutou fault (Tang, et al., 1976; Tsan, 1976; Lin & Lin, 1995). The area selected for this study was distributed between the Hsueshan Mountain Range zone and the Central Mountain Range zone geological area, and its northwest side was the Hsueshan Mountain Range zone. Its exposed strata comprised the Hsichun formation, Szuling Sandstone, and the Gangou Formation. Hsichun formation lithology is mainly cross-layers or alternate-layers with siltstone, hard shale, fine-grained metamorphic sandstones, and thick layer hard shale or slates with occasional metamorphic sandstones. Szuling Sandstone lithology mainly contains gray medium or coarse grains. Gangou Formation lithology mainly comprises argillite or slates with occasional thin layer fine meta-sandstone. The stratum exposed at the southeast side Central Mountain Range zone was the Lushan Formation, and its lithology mainly comprises thick layer grey-black slates (Fig. 1).

3 FEATURES OF AIRBORNE LIDAR TECHNOLOGY

Light Detection and Ranging (LiDAR), otherwise referred to as laser scanner or laser swath mapping technology, is a system that uses the laser beam distance measurement principle to conduct scan-type distance measurements. It has airborne and terrestrial systems. Airborne LiDAR or Airborne Laser Swath Mapping (ALSM) is based on the use of aircrafts as a vehicle and combines the laser system, the Global Positioning System (GPS), and the Inertial Navigation System (INS), as shown in Fig.2. When the data collected by integrating technologies is calculated or solved it can provide three dimensional coordinates of the terrain and ground objects (X, Y, Z). In addition to enabling quick and accurate terrain elevation measurement operations, it can also be used for analysis.

According to domestic and foreign airborne LiDAR technology application experiences, we can broadly summarize its characteristics shown as below: (1) High resolution and accuracy: in general, depending on varying mission planning, airborne LiDAR’s vertical accuracy is approximately 10 cm to 15 cm, and the horizontal accuracy is approximately 50 cm to 100 cm. (2) Data processing module automation: automated modules can be constructed for the steps of flight data acquisition and post-processing regardless of what system instrument is used. Unless specific high-specification results are required, general users can quickly and accurately obtain terrain data. (3) LiDAR reflection intensity data: besides elevation

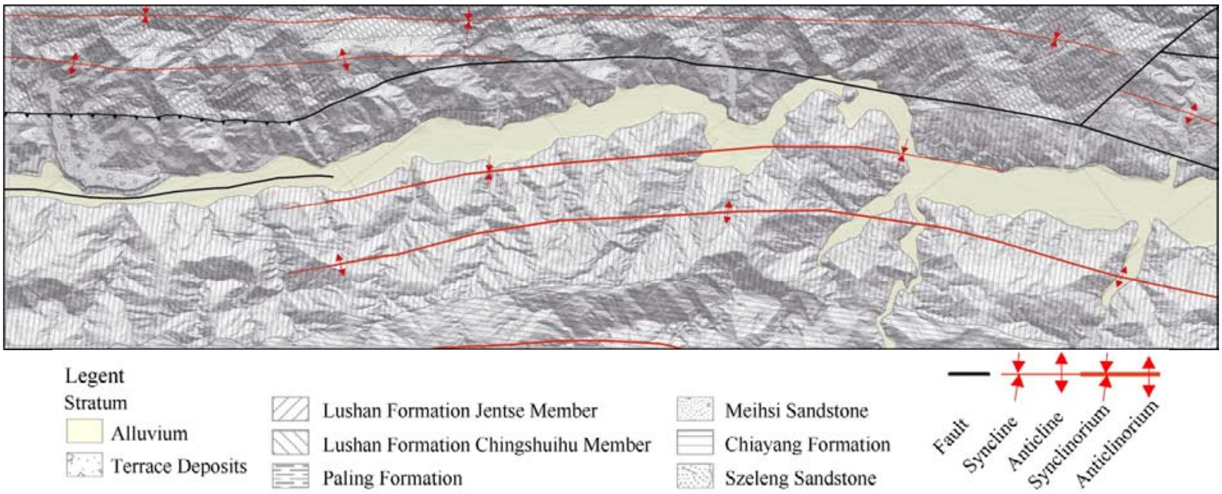

Fig. 1 Geological map of the study area (Geological Investigation and Database Construction for The Upstream Watershed of Flood-Prone Area-Geological Investigation, Landslide-Debris Flow Investigation and Their Suscepitability Evaluation in the Watershed Area of Central Geological Survey of China Taiwan)

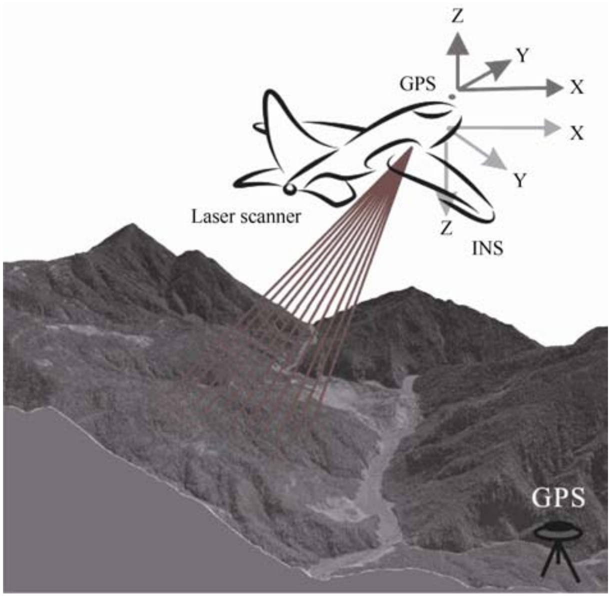

Fig. 2 Airborne LiDAR technology schematic

information, the laser reflection intensity is also recorded in the file and can be used to generate intensity images that react to the properties of the ground substances. (4) Ability to filter out vegetation or buildings: this is a unique advantage of the LiDAR system. Because LiDAR has multi-reflective features, it can provide the elevation data of the varying ground objects, filter out vegetation points or buildingswith numerical or digital processing, and can obtain actual ground andterrain feature or objectelevations. LiDAR's ability to provide actual ground elevations affords high levels of substantial assistance to geologists in all types of surveys and analysis, especially in the vegetation-filled terrain of Taiwan. (5) High density data points: because the emission frequency of the LiDAR laser is tens of thousands of times per second, it can collect extremely high-density reflection data within a very short period. These data can show subtle changes in the terrain surface after processing and can be used for investigation and analysis for the small gaps caused by fault scarp. (6) Simple ground control points: The GPS, inertial measurement, and laser distance measurement data for each airborne LiDAR laser measurement point arerecorded. Therefore, measuringwide area rangesrequires only few ground control points, which is convenient compared to traditional measurement methods.

4 RESULTS

4.1 LiDAR Digital terrain data

In this study, we used a BN-2B fixed-wing aircraft as the scanning vehicle. We conducted two LiDAR measurement missions before and afterthe typhoon season on June 22, 2008 (Fig.3) and October 31, 2008 (Fig. 4), respectively; we completed 29 routes of flight scanning measurements for the study region. The 2m-resolution DEM data for the study region were produced after the flight plan, scanning measurements, and point cloud data were processed. The results are shown in Fig. 3 and Fig. 4.

4.2 Digital Terrain Data Calculation and Analysis

We used the study region DEM data to conduct direct calculations and analysis and mainly employed ESRI ARCGIS software to obtain the elevation data and estimate terrain change amounts. The 2 m × 2 m grid method was employed to calculate or compute the DEM data and conducted sequential statistics on the elevation differences for the same location point (when X and Y had the same value). The result of the elevation difference values based on the scan data from the two different periods represented surface accumulation or erosion effects. Fig. 5 shows an overlay of the digital terrain data elevation difference value results on the terrain shadow map for after the typhoon season. The blue difference values were the accumulation areas, represented by positive value differences, and the red difference values were erosion areas, represented by negative value differences. In addition, we used different grid sizes to recalculate the average for the terrain elevation difference values; we enlarged the grid, making it equivalent to a 10 m × 10 m grid, for calculations (Fig. 6). Although the resolution was reduced, the system interpreted topographic changes for a larger area range.

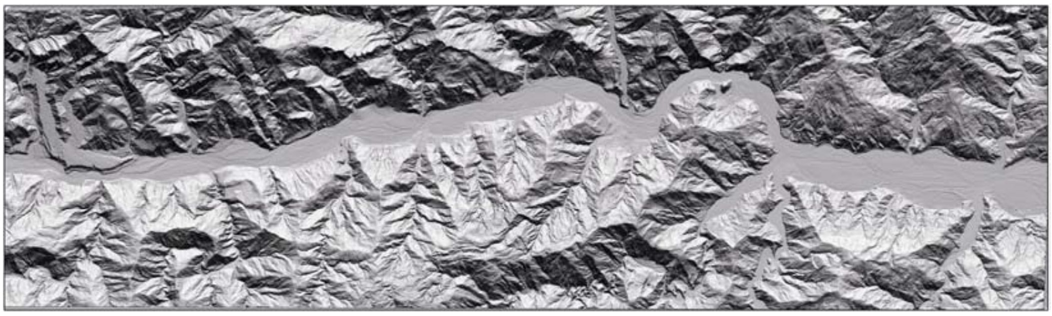

Fig. 3 LiDAR DEM shadow map of the study region scanned before the typhoon season

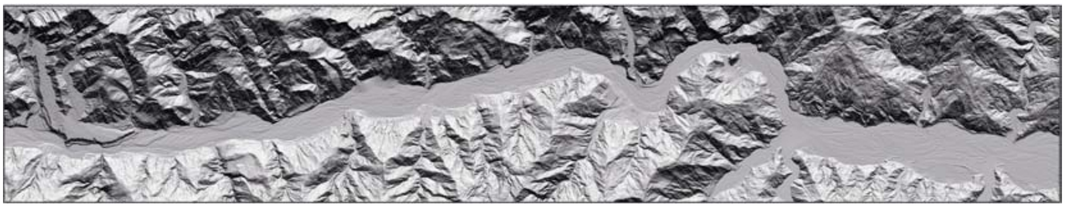

Fig. 4 LiDAR DEM shadow map of the study region scanned after the typhoon season

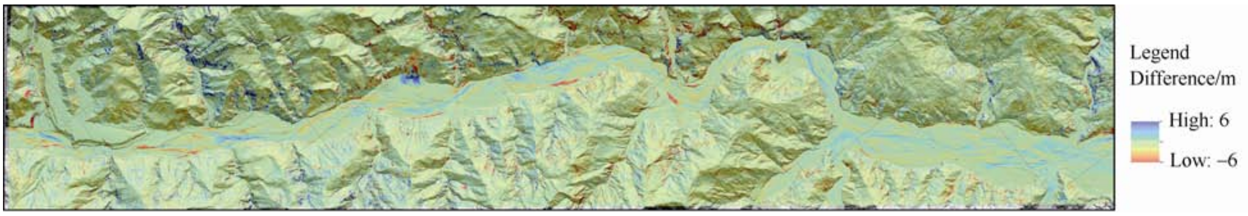

Fig. 5 Overlay of elevation difference values before and after the typhoon season on terrain shadow map for after the typhoon season

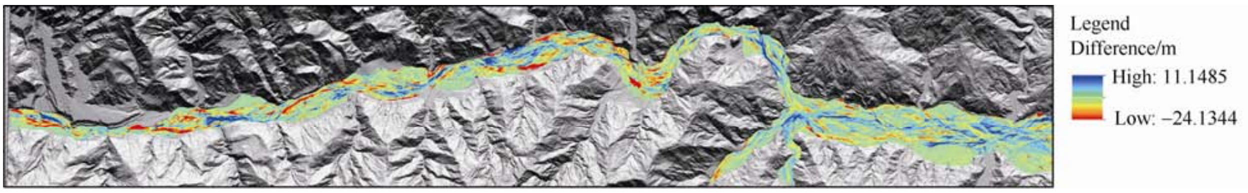

Fig. 6 River elevation difference values before and after the typhoon season (10 m grid) and post-typhoon terrain shadow map

5 DISCUSSION

5.1 Changes in the Lanyang River Channel During the Typhoon Season

Between July and September of 2008, the four major typhoon events discussed above produced large-scale, rapid, and concentrated heavy rainfall that significantly changed the Lanyang river terrain. Onsite observations can only detect these terrain changes to a limited scope and scale. For example, observations can only roughly outline washed out agricultural lands or eroded floodplains or river terraces in the river bed. Aerial photos or satellite images can detect the location and range of the terrain changes, but cannot accurately estimate or quantify the exact extent of the damages.

Comparing the terrains measured by airborne LiDAR technology before and after the typhoons, after the measured areas underwent four typhoons and heavy rain events, changes in terrain could be observed from the elevation difference values measured on two occasions overlaid on terrain shadow maps. For example, we clearly determined the extent and scope of the erosion for the floodplain and low river terraces of the main Lanyang River channels (Fig. 7). We could circle the exact extent of the elevation change amounts, including changes to the meandering main flow paths and the erosion changes to the floodplain and low river terraces. We could also interpret the position, scale, and elevation differences of the collapses caused by landslides on the slopes (Fig. 8). Taking the merging area of the Shitou Stream as an example, three tributaries flow into the main channel of the Lanyang River at this point. We determined the river terrace erosion and floodplain changes by examining the digital terrain data elevation difference value results for the two measurements (Fig. 9). By comparing the onsite photos (Fig. 10), we observed large-scale terrain changes. However, subtle terrain changes could only be detected and interpreted using the LiDAR digital terrain data.

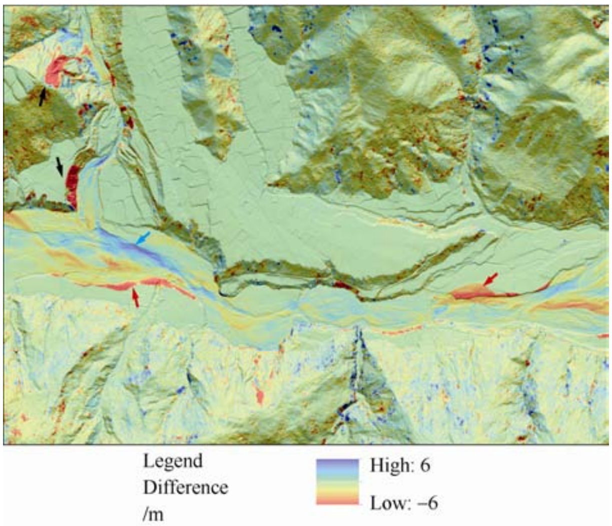

Fig. 7 Overlay of terrain elevation difference values of the Manoyuan region before and after the typhoon season on terrain shadow map(Blue represents accumulation, red represents erosion, the blue arrow shows river terrain accumulation change areas, the red arrows show floodplain areas impacted by erosion, and the black arrows showlandslides at the slope and terrace areas)

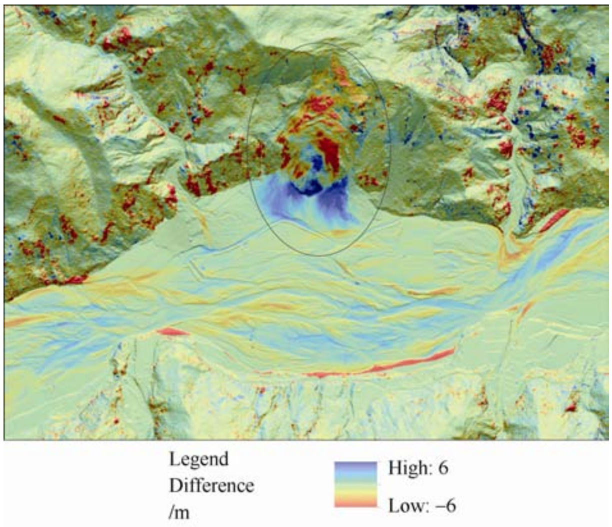

Fig. 8 Overlay of terrain elevation difference values of the Rumoan region before and after the typhoon season on terrain shadow map. The black oval indicates a landslide area

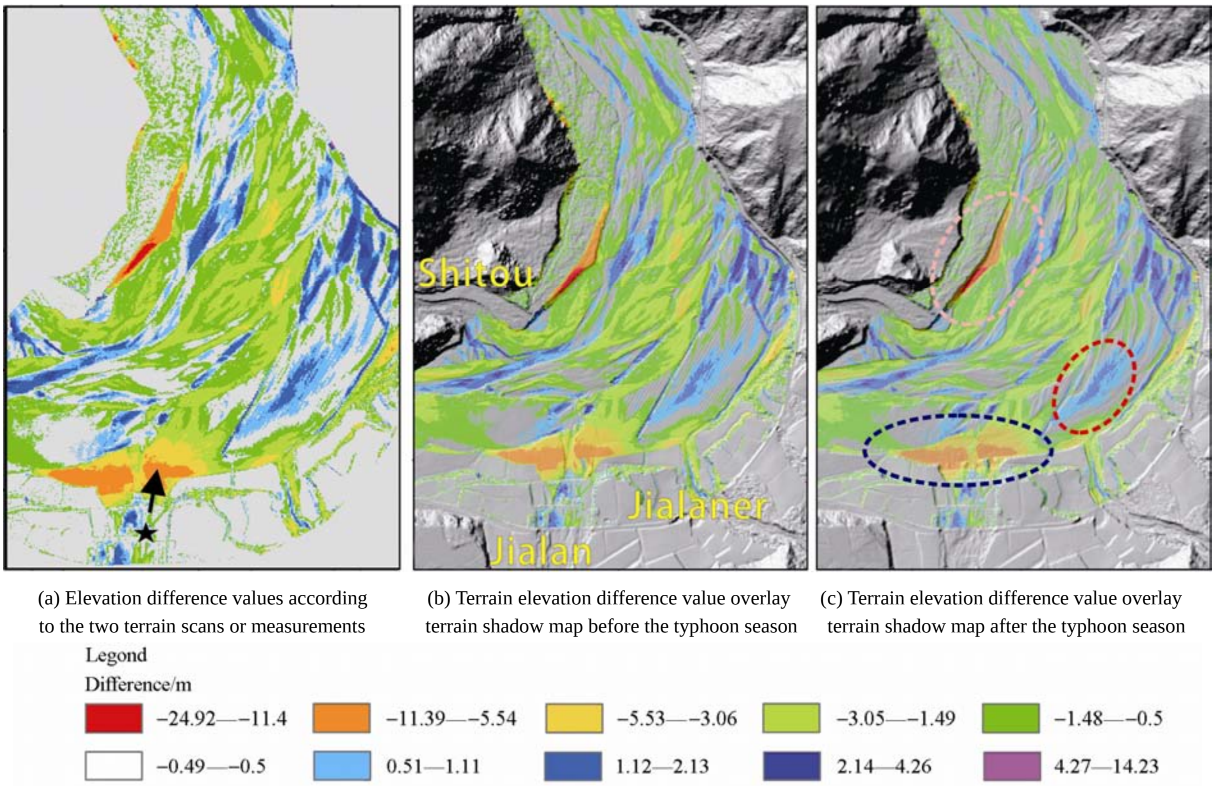

(a) Elevation difference values according to the two terrain scans or measurements (b) Terrain elevation difference value overlay terrain shadow map before the typhoon season (c) Terrain elevation difference value overlay terrain shadow map after the typhoon season

Fig. 9 Terrain elevation difference values and shadow maps before and after the typhoon season for the region where the Shitou, Jialan, and Jialaner Stream tributaries flow into the main Lanyang River Channel

5.2 River Deposit Transport Characteristics

We directly calculated and analyzed the resulting DEM data producedby the two flight missions before and after the typhoon season. We used ESRI ArcGIS software to project the terrain change amount using the elevation data obtained from two different periods based on the data of the two flight scan measurements. The $2\,\text{m} \times 2\,\text{m}$ grid method was used to compute the DEM data. The results showed the total amount of volume change for river channel erosion and accumulation transportation. The study region had a total erosion volume of more than 7300000 m^3, a total accumulation or deposit volume of more than 4900000 m^3, and the

(a) Shihtou stream (2007-09-14)

(b) Chialaner stream (2008-08-01)

(c) Chialan stream (2009-04-02)

Fig. 10 Site photos of the region where the Shitou, Jialan, and Jialaner tributaries flow into the main Lanyang River Channel before, during, and after the typhoon seasons (The location of the photos is indicated by the asterisk and arrow in Fig. 9(a))

total volume was reduced more than 2300000 m^3 of sediment. Following the various torrential rain incidents during the typhoon season, the Lanyang Riverwas predominately affected by erosion transportation, demonstrating that the study area was predominantly influenced by erosion and that the transportation effects caused more than 2300000 m^3 loses in sediment or debris.

5.3 Cross-sectional and longitudinal profile or section changes for the river

We horizontally divided the Lanyang River into a river profile based on different river channel characteristics and compared changes in the same locations before and after the typhoon season. Analyses for 35 areas were performed, and the profile locations are shown in Fig. 11. We projected the elevation profile data and relative locations before and after the typhoon, as shown in Fig. 12. We then calculated the terrain elevation difference value sum of the two measurements for the cross-sections. After reviewing the cross-sectional elevation difference value sum statistical charts, we determined that cross-section 13b was a critical dividing line. The results indicated that areas above 13a primarily showed erosion transport characteristics, and that the areas below 13b chiefly showed transport or accumulation transport characteristics.

From the cross-sections, the river transport characteristics were predominately affected by the slope, width, and curvature of the river, as well as the lithology of the two sides of the river. The main controlling factor of river transport is the slope of the river. Location 13b was a critical dividing line, as the river slope above 13b was significantly greater than below 13b (Fig. 13). This data indicated that the greater the slope of the river channel, the greater the erosion effects. River width and curvature were local influencing factors, and lithology distribution also affected the erosion and transport characteristics limited to the river valley and banks. Fig. 12 shows the river width change trends. The downstream area of the river tended to be wider. Comparison with data for river elevation difference value sums indicated that greater river width generally reflected stronger river accumulation transport characteristics. Terrain comparison before and after the typhoon seasons showed the river terrain changes between the dry and heavy rain seasons.

The longitudinal profile analysis of the Lanyang River was predominately based on terrain data from the past, pre-and post-typhoon season data collected by this study. The river channel was cut into vertical sections following the main flow for the Lanyang River main river channel (Fig. 14). The longitudinal profile displayed the slope trends of the river, which showed a similar slope trend for the study region. Unless there were significant changes to the terrain of the study region that were impacted by the entire river basin slope distribution, short-term typhoon changes did not cause obvious change impacts to the longitudinal profile of the river.

5.4 Lanyang Riverbed Sediment Transport Volume

The scouring and silting changes and the sediment transport volume of the riverbed play a critical role in soil and water conservancy, water conservancy planning, and ecological habitat changes. General riverbed sediment transport mechanisms can be divided into bedload and suspended load. Presently, analysis related to sediment transport volume is mainly based on the actual measurement data of the suspended load, flow volume of the

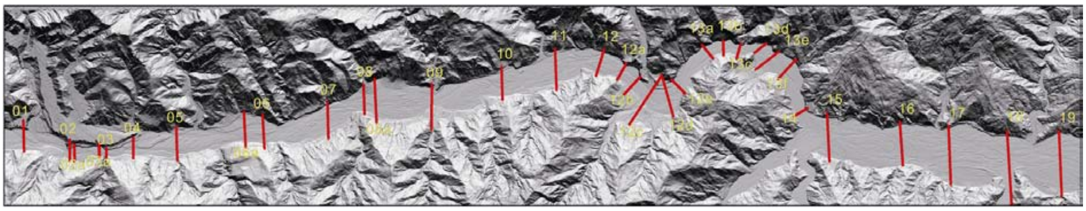

Fig. 11 Location map of the horizontally cut river channel cross-section areasfor the study region selected based on the different terrain characteristics of the river channel

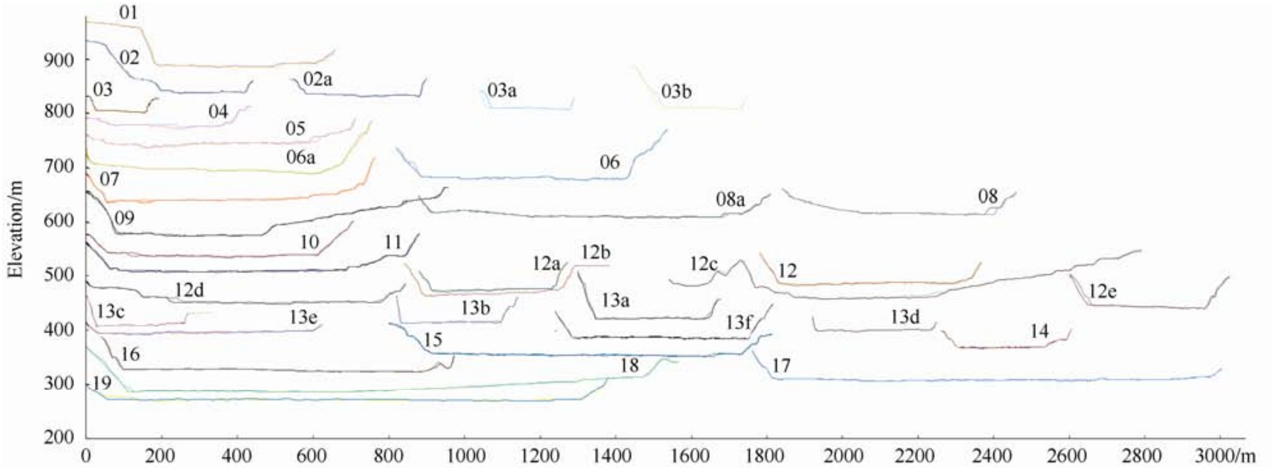

Fig. 12 The pre-and post-typhoon elevation cross-section data for two occasions for the 35 horizontal cross-sections of the Lanyang main river channel from Siji to Fanfan village

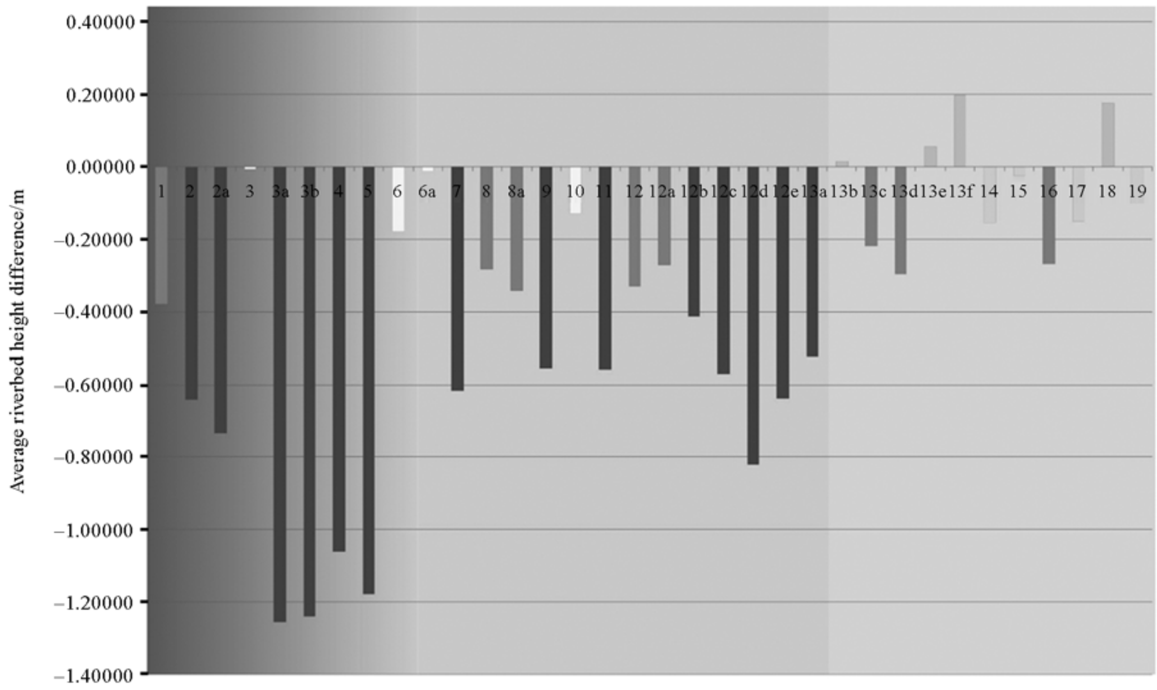

Fig. 13 Elevation difference value sum statistical charts for the cross sections

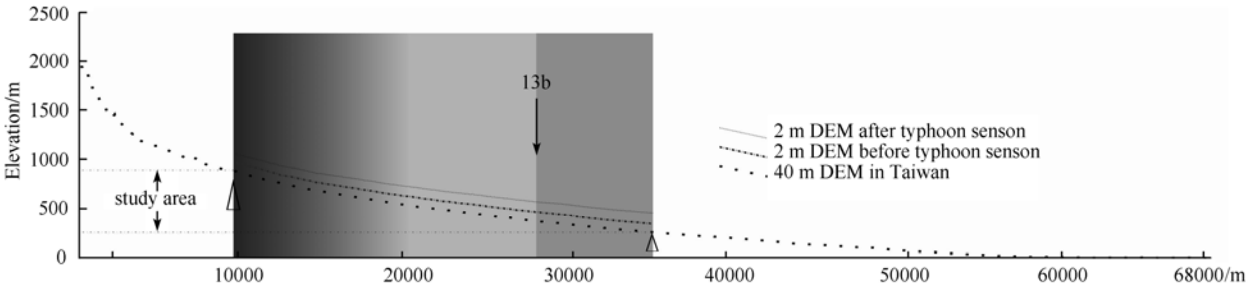

Fig. 14 Longitudinal profile of the Lanyang River based on various DEM data

hydrological station and the riverbed particle size analysis, and the hydrological analysis data. The empirical or theoretical formulae were used to calculate the total riverbed sediment transport (Chen, et al., 2007), but few actual measurements were produced. Furthermore, the inability to obtain the actual observed suspended load or particle size analysis during typhoon or heavy rain events also caused errors in the estimations.

Lin, et al. (2003) made calculations based on the average daily flow of the hydrological stations and suspended load production value, and found that suspended load in the upstream of the Lanyang River catchment are mainly affected by the transport influence of uncommon low-frequency high-flow events. That is, typhoon events are the most critical factors that affect the production of suspended load in the upstream catchment of the Lanyang River. Related studies in other regions of Taiwan (Chen, et al., 2007; Zhu, et al., 2007) also indicated that typhoon incidentsare a significant influencing factor of river suspended load production. Regarding the statistical data on Lanyang River sediment transport volume, Lin (2004) used a hydrological station flow duration hydrograph and a suspended load regression equation based on long-term hydrological station observation data and cross-sectional analysis to calculate the average annual sediment transport volume. Lin also considered how the flow rate of the upstream and downstream areas affected changes in the ratio of the suspended sediment or load and bedload to estimate the annual sediment transport volume statistical analysis for the main hydrological stations of the Lanyang River.

For the study region, we compared the Niutou Bridge hydrological station data collected by previous studies with the data collected by this study. The results indicated that after the four typhoon incidents in 2008, the volume of the river channels within the study region decreased by over 2350000 m^3. The 2008 hydrological data projected that the suspended load for the study area was over 2960000 m^3, the total sediment transport volume was over 5310000 m^3, and the ratio value for the bedload and suspended load was 9:11. If the changes in the sediment or debris volume of the river were viewed as changes in the volume of the bedload, and calculations were conducted based on the bedload and suspended ratio; using Taiwan’s past experience value of 1:5 for the calculations (Zheng, et al., 2005), the suspended load volume was greater than 11750000 m^3 and the total sedimentary volume was greater than 14100000 m^3. When a ratio of 3:7 was used (Dadson, et al., 2003), the suspended load volume was greater than 5483300 m^3 and the total sedimentary volume was greater than 7830000 m^3. If the 15% method was used (Lin, 2004), the suspended load volume was greater than 15666600 m^3 and the total sedimentary volume was greater than 18016600 m^3. A comparison of past study results (Lin, 2004; Kao, et al., 2001) showed that using the 3:7 ratio (Dadson, et al., 2003) is more reasonable and closer to the re-estimation results of Kao, et al., (2001). However, there were still differences compared to the projected ratio of 9:11 used in this study. The results indicated that the river sediment transport energy of the Lanyang River during heavy rainfall had been underestimated. Future water conservancy planning should reference this finding.

6 CONCLUSION

This study was the first of its kind to use the airborne LiDAR system to measure river terrain data for a large watershed area. It also created different periods of digital terrain data before and after a typhoon season. We used the elevation difference value topography measurement method to calculate the Lanyang River terrain changes before and after a typhoon season. The results of the study showed that the airborne LiDAR high resolution digital terrain model data produced excellent results when used to calculate river terrain and sediment volume changes or change amounts.

After the Lanyang River channel experienced four typhoons in 2008, we directly calculated and analyzed the resulting digital terrain model data generated by two flight missions before and after the typhoon season, and used the elevation data collected for two different periods to estimate the terrain change amounts based on data measured by the two aerial scans. The results indicated that the study region was predominately affected by erosion, and that sediment transport loss volume was greater than 2300000 m^3.

The cross-sectional elevation difference value sum data of the study region indicated that areas above Fig. 13(a) showed the upstream erosion segment and midstream transport segment characteristics, and areas below Fig. 13(b) showed mainly midstream transport segment characteristics. The main controlling factor of river transport is the slope of the river. The greater the slope of the river channel, the more obvious the effects of erosion. River width and curvature cause local effects, and lithology distribution also affected the erosion and transport characteristics limited toriver valleys and banks.

The results indicated that after the four typhoons in 2008, the volume of the river channels within the study region decreased by over 2350000 m^3. If the river debris or sediment volume change amount can be considered the bedload change amount, based on 2008 hydrological data, the suspended load for the study area was over 2960000 m^3, the total sediment transport volume was over 5310000 m^3, and the ratio value of the bedload and suspended load was 9:11. These results indicated that the sediment transport energy of the Lanyang River during heavy rain had been underestimated. Future water conservancy planning should reference this finding.

REFERENCES

Brasington J, Langham J and Rumsby B. 2003. Methodological sensitivity of morphometric estimates of coarse fluvial sediment transport. Geomorphology, 53(3–4): 299–316 [DOI: 10.1016/S0169-555X(02)00320-3]

Cavalli M, Tarolli P, Marchi L and Dalla Fontana G. 2008. The effectiveness of airborne LiDAR data in the recognition of channel-bed morphology. Catena, 73(3): 249–260 [DOI: 10.1016/j.catena.2007.11.001]

Chen H L and Chang J C. 2007. The discharge and sediment load of heavy rainfall events in the tsengwen river basin, southern Taiwan. Journal of Geographical Science, (48): 43−65

Dadson S J, Hovius N, Chen H, Dade W B, Hsieh M L, Willett S D, Hu J C, Horng M J, Chen M C, Stark C P, Lague D and Lin J C. 2003.

Links between erosion, runoff variability and seismicity in the Taiwan orogen. Nature, 426(6967): 648–651 [DOI: 10.1038/nature02150]

Ho C S. 1986. An introduction to the geology of Taiwan explanatory text of the geologic map of Taiwan. 2nd edition. China Taiwan: China Taiwan Central Geological Survey Publishing house: 164

Kao S J and Liu K K. 2001. Estimating the suspended sediment load by using the historical-Hydrometric record from the Lanyang-His watershed. TAO, 12(2): 401–414

Lane S N and Richards K S. 1998. High resolution, two-dimensional spatial modelling of flow processes in a multi-thread channel. Hydrological Processes, 12(8): 1279–1298 [DOI: 10.1002/(SICI)1099–1085(19980630)12:8<1279::AID-HYP615>3.0.CO;2-E]

Lane S N, Richards K S and Chandler J H. 1994. Developments in monitoring and modelling small-scale river bed topography. Earth Surface Processes and Landforms, 19(4): 349–368 [DOI: 10.1002/esp.3290190406]

Lane S N, Westaway R M and Murray Hicks D. 2003. Estimation of erosion and deposition volumes in a large, gravel-bed, braided river using synoptic remote sensing. Earth Surface Processes and Landforms, 28(3): 249–271 [DOI: 10.1002/esp.483]

Lin C W, and Lin W H. 1995. A study on the geological structures of the Lanyangchi area, northern Taiwan. Bulletin of China Taiwan Central Geological Survey, 10: 23–49

Lin C Y. 2004. Discussion on Sediment sources and downstream of river erosion and deposition in Lanyang River, The life history of Lanyang River: Ilan Research, 113–129

Milan D J, Heritage G L and Hetherington D. 2007. Application of a 3D laser scanner in the assessment of erosion and deposition volumes and channel change in a proglacial river. Earth Surface Processes and Landforms, 32(11): 1657–1674 [DOI: 10.1002/esp.1592]

Rumsby B T, Brasington J, Langham J A, McLelland S J, Middleton R and Rollinson G. 2008. Monitoring and modelling particle and reach-scale morphological change in gravel-bed rivers. Applications and Challenges Geomorphology, 93(1-2): 40–54 [DOI: doi:10.1016/j.geomorph.2006.12.017]

Wheaton J M, Brasington J, Darby S E and Sear D A. 2010. Accounting for uncertainty in DEMs from repeat topographic surveys: improved sediment budgets. Earth Surface Processes and Landforms, 35(2): 136–156 [DOI: 10.1002/esp.1886]

Wu Y C. 1976. The geology of geothermal energy area in Chingshui–Tuchang. Mining Technology, 14: 484–489

Chiang Y S, Chen K S, Liang L S and Wang C T. 2007. Prediction of sediment yield using SPOT imagery and digital terrain model. Journal of Photogrammetry and Remote Sensing, 12(4): 447–456

Tsan S F. 1976. The folding and block movement of The Hsuehshan Range, Taiwan. Bulletin of Central Geological Survey of China Taiwan, 25: 29–34

Cheng C T, Ku C Y, Chou H C, Chang Y L and Chern J C. 2005. The estimation of catchment sediment budget by usingremote sensing methods. Sinotech, (87): 1–5

Tang C H and Yang C Y. 1976. Mid-Tertiary stratigraphic break in the northeast Hsuehshan Range of Taiwan. Petroleum Geology of China Taiwan, 13: 139–147

Chu I T and Hsu M L. 2007. The relationship between discharge and suspended sediment concentration at typhoon events in Yu-Feng Catchment. Journal of Geographical Science, (49): 1–22

激光雷达地形资料用于河道输沙的研究

谢有忠[1,3]，詹瑜璋[2]，胡植庆[1]，林朝宗[3]

1. 中国台湾大学地质科学系，中国台湾 10617；
2. 中国台湾地球科学所，中国台湾 11581；
3.中国台湾地质调查所，中国台湾 23585

摘 要：中国台湾地区位处亚热带地区，夏季受台风暴雨侵袭，加上位处板块运动活跃处，造成地形变化较大，尤其在台风暴雨后河道地形都会产生很大的变化；目前航空激光雷达地形数据，分辨率较高、精度、便利性，并可以滤除建筑物与树木遮蔽，还原原始地面形貌，符合地质与地形分析研究的需要。2008 年兰阳溪地区经历海鸥(KALMAEGI)、凤凰(FUNG-WONG)、森拉克(SINLAKU)、蔷薇(JANGMI)等 4 次重大台风事件，河床地形变化甚剧，因此本研究利用两次航空激光雷达测量地形数据，分析比较台风前后河床地形以及河道输沙的变化。研究成果首次展示空载激光雷达系统，在大流域面积测量河道地形应用效果显著，于台风季节前后产制不同时期的数值地形数据，并应用高程差值的地形计量方法，计算在台风季节前后河道地形的变化，研究结果显示空载激光雷达高解析数值地形模型数据，应用在河道地形变迁与沉积物体积变化量计算，可以得到极佳的成果。

关键词：兰阳溪流域，台风暴雨事件，地形特征，航空激光雷达，数值地形模型

中图分类号：TP95　　**文献标志码**：A

引用格式：谢有忠，詹瑜璋，胡植庆，林朝宗．2013．激光雷达地形资料用于河道输沙的研究．遥感学报，17(1): 193–209
Hsieh Y C, Chan Y C, Hu J C, Lin C C. 2013. Using LiDAR DTMs data for river sediment transport. Journal of Remote Sensing, 17(1): 193–209

1 引 言

中国台湾地区位处亚热带地区，夏季受台风暴雨侵袭，加上位处于板块运动活跃处，地质构造活动一直持续中，造成地形变化甚剧，尤其是在台风暴雨后河道的地形都会产生很大的变化；兰阳溪为台湾地区主要河川之一，夏季很容易直接受到来自太平洋形成之台风暴雨侵袭，进而发生上游地区自然冲蚀、崩塌，产生的土沙随径流往下游河道输运，而造成中下游地区河床淤高、掏刷或河道变迁等现象。台湾地区各大河川的年输沙量多在 6000 t/km^2 以上，兰阳溪年泥沙产量甚至超越 40000 t/km^2，对于水土保持、水利工程规划、河道生态栖地变化等产生影响，有关河床地形变化及输沙量的统计研究极为重要。

数值高程模型(DEM)在地质与地形学的领域可以提供极佳的应用，可依需要呈现平面或立体的模型，有效展现不同角度的地形特征。数值地形模型的取得方法，从地形等高线、侧视激光雷达、卫星影像、航测空照、实时动态差分全球定位系统 RTKGPS (Real Time Kinematic GPS)、全测站经纬仪测量(Total Stations)、激光雷达系统(航空 Airborne LiDAR、地面 Terrestrial LiDAR)等等，随着技术的进步，精度和分辨率也一直提升，许多地形计量方法和成果，陆续由地形数据的提升而呈现更进步的成果。在河流地形研究，以往数值地形数据主要应用在河道地貌、河流横剖面、纵剖面等变化的分析(Lane 和 Richards, 1998)，从 1990 年开始利用不同时期的地形测量所获取的数值地形模型数据，除建构不同时期的河道地形，并利用不同时期地形变化的高程差值，进一步发展不同的河道地形计量(Lane 等, 1994; Brasington 等, 2003; Lane 和 Richards, 1998; Lane 等, 2003; Milan 等, 2007; Rumsby 等, 2008; Wheaton 等, 2010)，由河道地形变化

收稿日期：2012-01-15；**修订日期**：2012-08-24

第一作者简介：谢有忠(1974—)，男，博士研究生，主要从事环境地质调查及遥测技术在地质灾害的应用研究。 E-mail:spencer1121@gmail.com

通信作者简介：詹瑜璋(1966—)，男，研究员，主要从事构造地质学、新构造运动学、遥测地质学等相关研究。 E-mail: yuchang@earth.sinica.edu.tw

的高程差值可以了解河道堆积以及侵蚀的区域范围，并可实际推算河道中侵蚀和堆积的体积变化，综合推算出河道地形变迁的总体积变化。而上述文献中多数利用航测、RTK GPS 等技术所产出的数值地形模型数据来计算，其方法除研究范围有限，多介于数平方公里间，且不同技术间的误差差异也增加地形变迁计算上的复杂变量。利用不同时期的航空激光雷达系统技术，可实际应用于更大面积的流域或崩塌地监测分析(Cavalli 等，2008)。在台湾地区也有利用风灾前后拍摄航测所产生的数值地形模型，分析计算风灾前后的 DTM 差异，进而推算可能的土沙产量(郑锦桐 等，2005)，与利用 SPOT 影像及 DTM 推估泥沙产量(江阳圣 等，2007)。

2008 年 6 月完成兰阳溪中上游部分地区的激光雷达数值地形测制后，兰阳溪地区随即经历海鸥、凤凰、森拉克、蔷薇等 4 次重大台风事件，河床地形变化大，因此本研究于相同河道范围约 100 km^2，在 2008 年 10 月再次进行航空激光雷达地形的测量，首次应用航空激光雷达系统在大流域面积测制河道地形，并在台风季节前后制作不同时期的数值地形数据，应用高程差值的地形计量方法，来计算兰阳溪在台风季节前后地形的变化，分析比较台风事件前后河床地形以及河道输沙的变化。

2 研究区域概况

本研究选择兰阳溪中上游区域，兰阳溪原名宜兰浊水溪，以含沙丰富、水质混浊而得名，为台湾地区主要河川之一，也为台湾地区东北部宜兰县境内最大河川，发源于南湖大山北麓。兰阳溪自发源地开始，蜿蜒于雪山山脉与南湖大山山脉之间，本溪流向东北流至破布乌始入平地，溪流分支成网状乱流，至兰阳大桥附近形成干流，再向东流后注入太平洋，流域面积约 978 km^2，主流长度约 73 km。

主流兰阳溪系属急流河川，上游坡陡流急，洪水期常挟带大量泥沙下泄，且雨量集中，洪水流量颇大，冲击破坏的能力甚强。历年常受洪水主流直冲而发生灾害，以致堤防护脚、基脚遭洪流刷深，或因堤防坡面受洪水土石磨损冲击损毁而酿灾。

研究区域位于兰阳溪中上游流域英士至四季一带(图 1)，由于研究区域位居台湾地区东北部中央山脉与雪山山脉地区，在遥感影像中兰阳溪主河道呈现明显一线型，此线型由牛斗附近向南南西方向延伸至兰阳溪上游，过去许多地质工作者多将此一线型称为梨山断层(何春荪，1986；吴永助，1976)或牛斗断层(汤振辉 等，1976；詹新甫，1976；曾长生等，1975；林启文和林伟雄，1995)，本研究区域刚好分布于雪山山脉带和中央脊梁山脉带地质区，西北侧属于雪山山脉带，出露地层包含有西村层、四棱沙岩和干沟层，西村层岩性以粉沙岩质硬页岩与细粒变质沙岩的互层、厚层硬页岩或板岩偶夹变质沙岩为主，四棱沙岩岩性以灰色中粒至粗粒，干沟层岩性主要以硬页岩或板岩为主，偶夹薄层之细沙岩，东南侧中央脊梁山脉带出露地层主要为庐山层，岩性以厚层灰黑色板岩为主(图 1)。

3 航空激光雷达技术的特点

激光雷达或称雷射测距扫描技术(Laser Scanner; Laser Swath Mapping)，为利用激光束测距原理进行扫描式测距的系统。主要可以包含航空及地面两种系统。

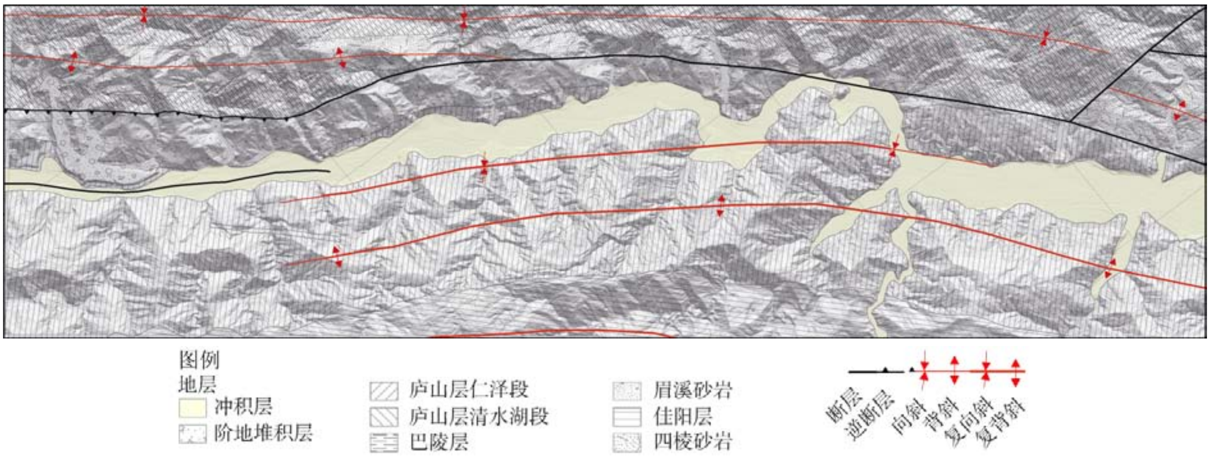

图 1 研究区域地质图(中国台湾地质调查所的易淹水地区上游集水区地质调查及数据库建置—集水区地质调查及山崩土石流调查与发生潜势评估成果报告)

航空激光雷达系以航空器为载具，结合激光雷达系统、全球定位系统 GPS 与惯性导航系统 INS (Inertial Navigation System) (图 2)，将 3 种技术整合，并获取数据加以解算后，即可得地形地物之 3 维坐标(*X*、*Y*、*Z*)，除使得地形高程测量作业更快速而准确，且能进一步应用分析。

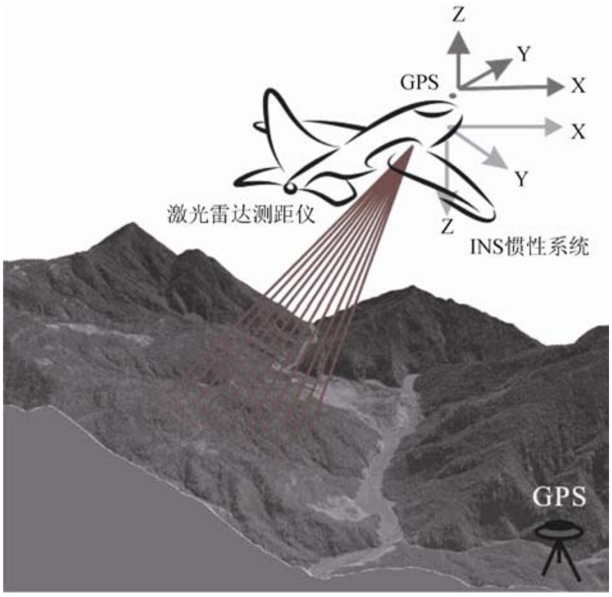

图 2　航空激光雷达技术示意图

航空激光雷达技术的特性主要有：(1)分辨率及准确性高：依据不同任务规划，一般而言，航空激光雷达在垂直方向的准确度大约是 10—15 cm，在水平方向的准确度则约为 50—100 cm；(2)数据处理模块自动化：飞航数据采集与后制处理，不论使用何种系统仪器，其步骤都可以建立自动化模块，除了需特定高规格成果外，一般用户可以快速且正确地获取地形资料；(3)激光雷达反射强度数据：除了高程数据之外，激光雷达反射强度也记录于档案中，可用来产生强度影像，反应地面物质的性质；(4)有滤除植被或建物的能力：这也是激光雷达系统的特别优点，因为激光雷达具有多重反射特性，可提供不同地物的高程，再以数值处理滤掉植被点或建物，便可以得到地面真实高程及地物高程；尤其在台湾地区多植被地形，激光雷达提供真实地面高程对地质学家在各方面的调查分析都有极大帮助；(5)高密度数据点：由于激光雷达系统激光所发射频率为每秒数万次，可在很短的时间内收集到密度相当高的反射数据。这些数据经处理后可表现地形的细微变化，能应用在调查分析断层崖造成的微小落差；(6)地面控制点简易：就航空激光雷达而言，每个激光雷达测点皆有记录全球卫星定位数据、惯性测量数据与激光雷达所测得的距离，因此在大范围区域测量，只要有几个地面控制点即可，比起传统测量方便许多。

4　研究成果

4.1　激光雷达数值地形资料

本研究使用 BN-2B 定翼机作为扫描载具，在台风季节前分别进行 2 次激光雷达测量，日期分别为 2008-06-22 (图 3)以及 2008-10-31(图 4)，完成研究区域内共计 29 条航线的飞航扫瞄测制。经飞航规划、扫瞄测制以及点云数据处理后，产生研究区域范围的 2 m 分辨率数值地形模型(DEM)数据，成果如图 3 及图 4 所示。

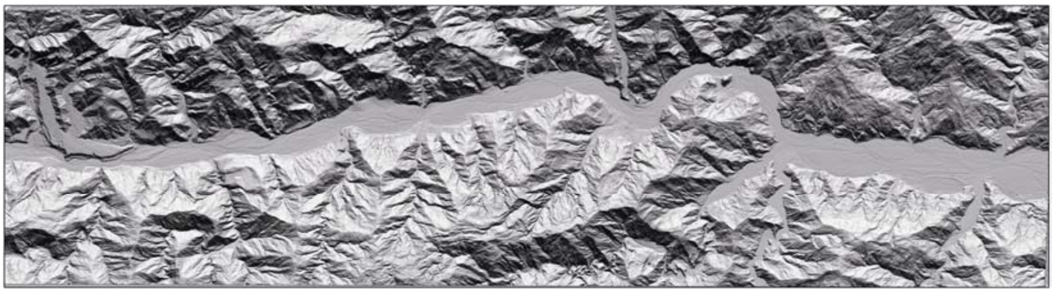

图 3　研究区域台风季节前扫瞄 LiDAR DEM 阴影图

图 4　研究区域台风季节后扫瞄 LiDAR DEM 阴影图

4.2 数值地形数据计算分析

利用研究区域范围 DEM 数据直接计算分析，主要使用 ESRI ARCGIS 软件，以获取高程数据推估地形变化量，数值地形模型数据以 2 m×2 m 网格方式运算，将相同位置点(X，Y 值相同)高程差依序统计。两次不同时间获取的高程数据差值结果，表示地表堆积或侵蚀作用，图 5 为数值地形资料高程差值结果迭置台风季节后地形阴影图，差值蓝色表示正值，为堆积区域，差值红色表示负值，为侵蚀区域。另外利用不同网格大小重新计算地形高程差值平均，将网格放大相当于以 10 m×10 m 网格方式运算(图 6)，虽然分辨率降低，但可以适时反应较大范围之地形变化判释。

5 讨 论

5.1 台风季节兰阳溪河道变化

2008 年 7 月到 9 月之间，兰阳地区历经前述的 4 次重大台风，大规模且快速集中的大雨，让兰阳溪的河道地形产生明显变化，而从这些地形变化的现场实际观察仅能于一定范围、规模以上观测出变化，如河床中被冲毁农地或受侵蚀的高滩河阶，也只能约略概述，如果利用航空影像或卫星影像，或可发现地形变化的位置及范围，但仍无法确切估算或量化损害程度。

利用航空激光雷达技术在台风前后所测量的地形比对后，本研究测量范围的地形的变化可从两次测量的高程差值迭置地形阴影图观察出，如兰阳溪主河道可以清楚判释出高滩地和低位河阶受侵蚀的程度和范围(图 7)，包括蜿蜒主水流路径变化、高滩地和低位河阶受侵蚀变化，都可以明显地圈绘出确切范围及高差变化量。坡面上发生的崩塌地，也可清楚地判释，包含崩塌的位置、范围和崩落的高程差(图 8)。以石头溪汇入口为例，3 条支流恰于此处汇入兰阳溪主流，河阶地的侵蚀和河道高滩地的变迁都可以经由两次测量的数值地形资料高程差值结果判释图 9，对照现场

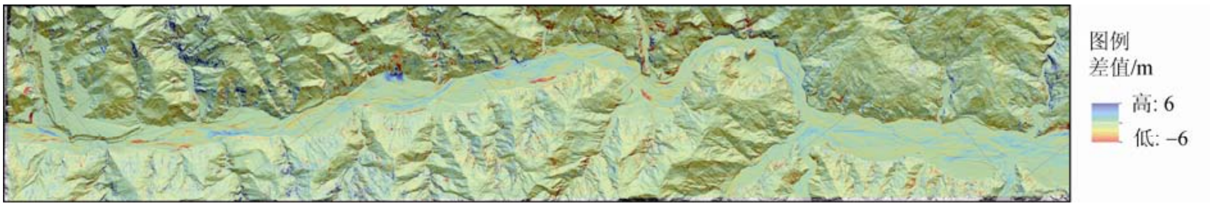

图 5 台风季节前后高程差值迭置台风季节后地形阴影图

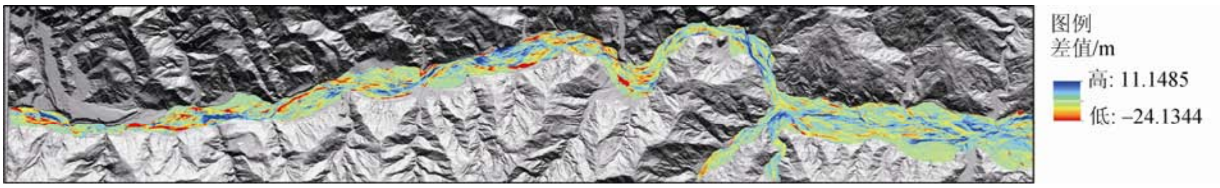

图 6 台风季节前后河道高程差值(10 m 网格)与台风季节后地形阴影图

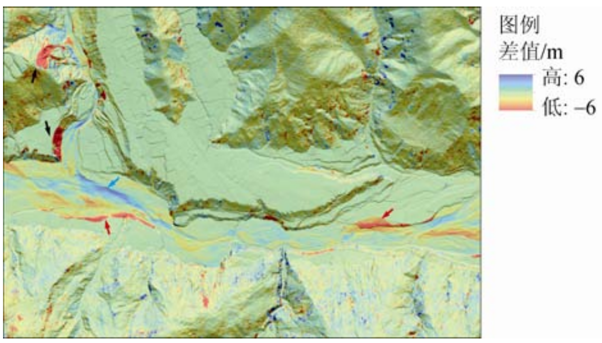

图 7 马诺源地区台风季节前后地形高程差值迭置地形阴影图(其中蓝色为堆积、红色为侵蚀，蓝色箭头为河道地形堆积变迁处，红色箭头为高滩地受侵蚀影响处，黑色箭头为坡面及阶地周围崩塌地)

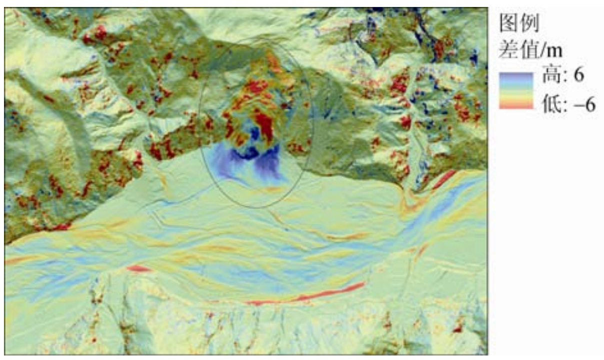

图 8 留茂安地区台风季节前后地形高程差值迭置地形阴影图，黑色椭圆范围为一处崩塌地

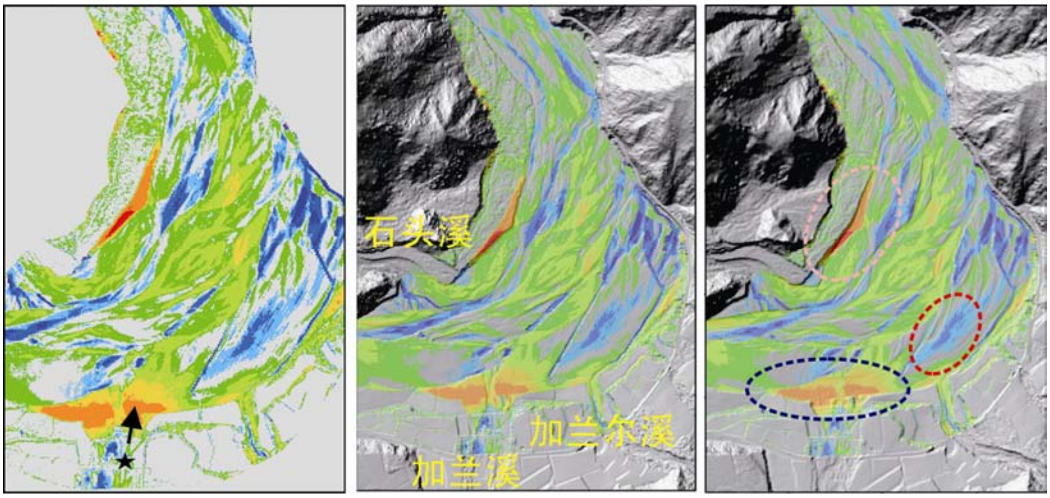

(a)两次测量地形之高程差值　　(b)将地形高程差值迭置台风前之地形阴影图　　(c)将地形高程差值迭置台风后之地形阴影图

图例
差值/m

−24.92—−11.4	−11.39—−5.54	−5.53—−3.06	−3.05—−1.49	−1.48—−0.5
−0.49—−0.5	0.51—1.11	1.12—2.13	2.14—4.26	4.27—14.23

图 9　石头溪、加兰溪及加兰尔溪等支流汇入兰阳溪主流范围，地形高程差值与台风季节前后的地形阴影图

照片(图 10)也可观察出较大规模的地形变化，但较细微的地形变化，则需利用激光雷达数值地形数据才可判释。

5.2　河道堆积物搬运特性

利用台风季节前后两次飞行任务的结果，所产生的数值地形模型数据直接计算分析。使用 ESRI ArcGIS 软件，将两次飞航扫瞄测量的数据，运用两次不同时间所获取的高程数据推估地形变化量，数值地形模型数据以 2 m×2 m 网格运算，显示河道侵蚀堆积搬运的体积变化总量，本研究区域内侵蚀体积量共约 730 万 m^3，堆积体积量共约 490 万 m^3，整个体积共减少约 230 余万 m^3，经过台风季节的数次暴雨事件，兰阳溪河道主要受侵蚀搬运所影响，显示研究区域内仍主要受侵蚀影响，搬运作用流失高达 230 余万 m^3 的土石量。

5.3　河道横剖面与纵剖面变化

将兰阳溪针对河道不同特征处横切河道剖面，比对同一位置在台风季节前后变化，共分析 35 处，剖面位置如图 11 所示，并将台风前后高程剖面数据及相对位置投影至图 12，另将横剖面两次测量的地形高程计算差值和，由横剖面高程差值和统计图检阅，横剖面图 12 中 13b 为一重要分界位置，显示 13a 以上主要以侵蚀搬运特性为主，13b 以下则开始以搬运或堆积搬运为主的特性。

(a) 石头溪(2007-09-14)

(b) 加兰尔溪(2008-08-01)

(c) 加兰溪(2009-04-02)

图 10　石头溪、加兰尔溪及加兰溪等支流汇入兰阳溪主流范围台风季节前、中、后不同时期的照片(照片拍摄地点、方向为图 9(a)的星号及箭号方向)

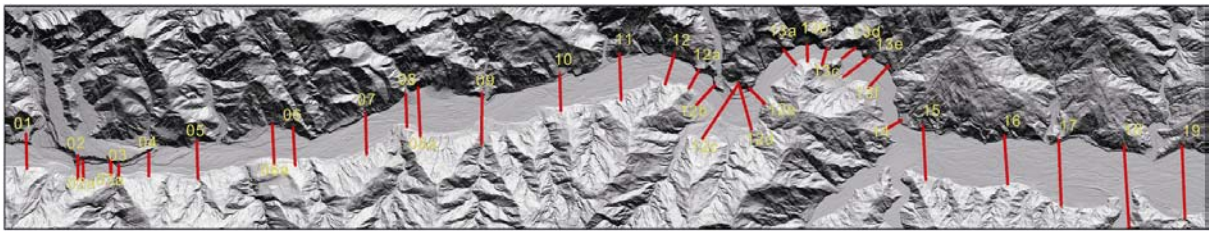

图 11 研究区域内不同地形特征河道的横切剖面位置图

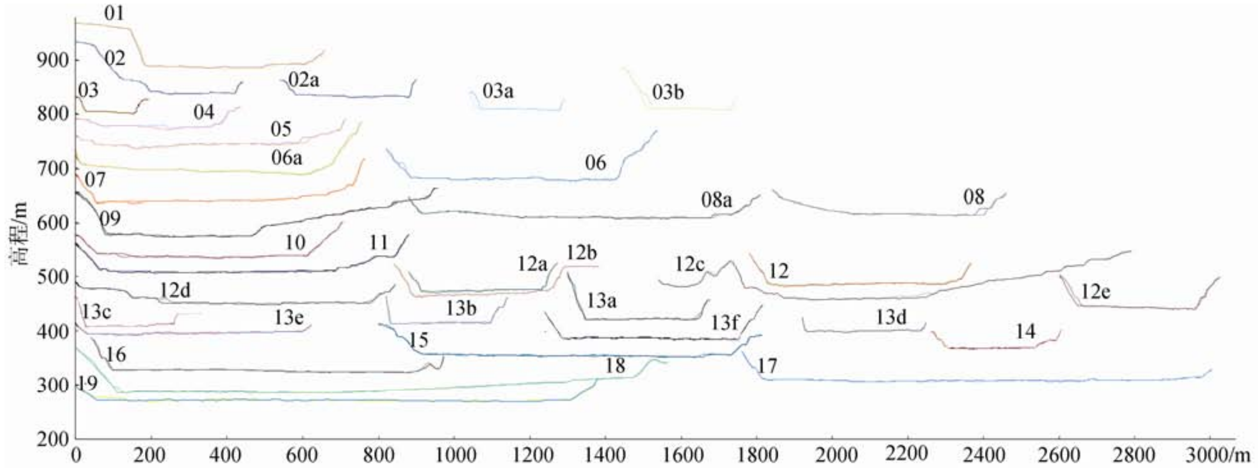

图 12 兰阳溪主河道自四季至梵梵共 35 横剖面，台风前后两次的高程横剖面资料

河道搬运特性由所有横剖面来看，应该主要受到河道坡度、河道宽度、河流曲率、河道两侧岩性等因素影响。河道搬运主要的控制因素应为河道坡度，上述中图 12 中 13b 为一重要分界，13b 以上之河道坡度明显大于 13b 以下(图 13)，显示河道坡度越大，侵蚀作用越明显；局部则受河道宽度及河流曲率影响，而岩性分布也影响受限河谷及河道两岸侵蚀、搬运的特性，由图 12 来看河道宽度的变化趋势，河道宽度越往下游有变宽的趋势，与河道高程差值和的资料比对，河道宽度越宽，多数反应河道堆积搬运的特性。另外由台风前后的地形比对，也可观察枯水期间与暴雨期间的河道地形变迁。

兰阳溪纵剖面分析，主要利用过去地形数据以及本研究台风季节前后的数据等，沿着兰阳溪主河道主水流槽线纵切河道剖面(图 14)，纵剖面显示为河道坡度趋势，可见研究区域内河道坡度趋势相当接近，除非区域内地形有重大改变，而受到整个流域河道坡度分布影响，短时期台风变化对纵剖面并不会有明显变化影响。

5.4 兰阳溪河床输沙量

河床冲淤变化、输沙量，在水土保持、水利工程规划、河道生态栖地变化等都扮演着重要角色，一般河床中土沙输运的机制大致可分为底床载(bedload)、悬浮载(suspencded load)两种，目前有关输沙量的分析多以实测悬浮载观测资料、水文站流量配合河床质粒径分析及水文分析数据，利用经验公式或理论公式进而推算出河床总输沙量(陈翰霖和张瑞津，2007)，实测值较少。加上在台风、暴雨时，无法获取实际观测悬浮载或粒径分析等，也将造成推估上的误差。

林致远(2004)以水文站日平均流量及悬移质生产值计算，显示兰阳溪上游集水区的悬移质主要受到不常发生的低频率高流量事件的搬运影响，也就是说台风为影响兰阳溪上游集水区悬移质生产最重要的因素，在台湾其他地区相关研究(陈翰霖和张瑞津，2007；朱怡亭和徐美玲，2007)也显示台风事件对河川悬移质生产占很大影响因素。有关兰阳溪输沙量统计资料，林致远(2004)主要以长期水文站观测数据及断面分析，利用水文站流量延时历线与悬移质回归方程式计算平均年输沙量，并考虑上、下游流速影响造成悬移质与推移质的比例变化，进而推算出兰阳溪主要水文站年输沙量统计分析。

以本研究区域而言，可取用前人以牛斗桥水文站

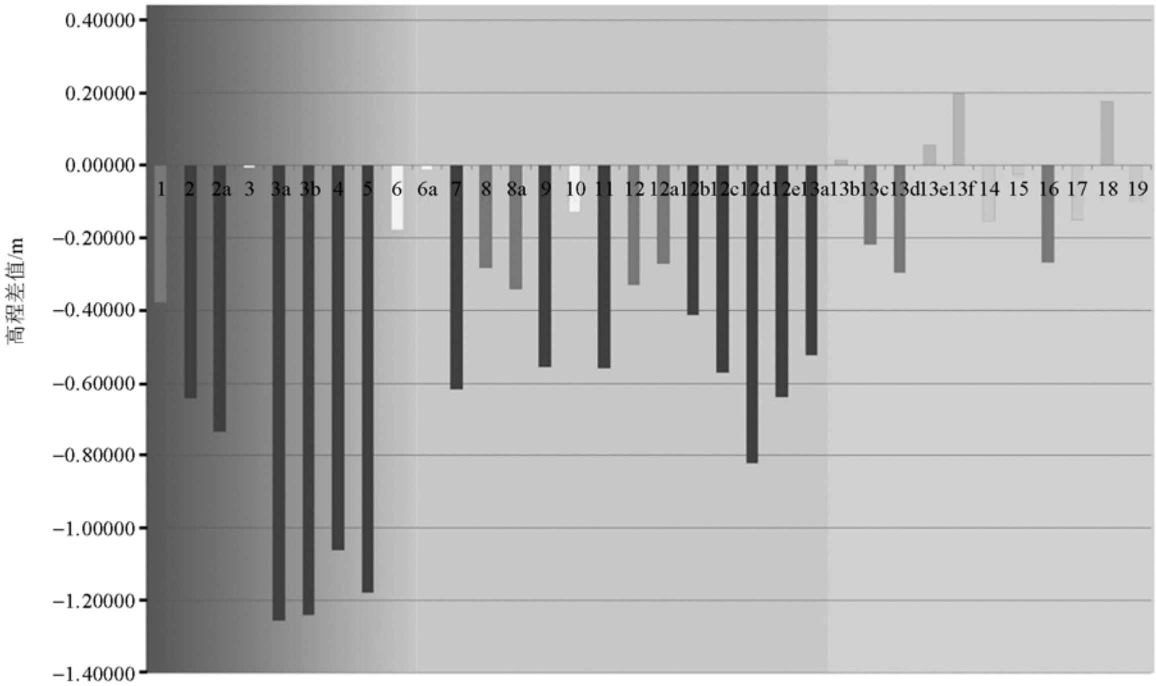

图 13 横剖面的高程差值和统计图

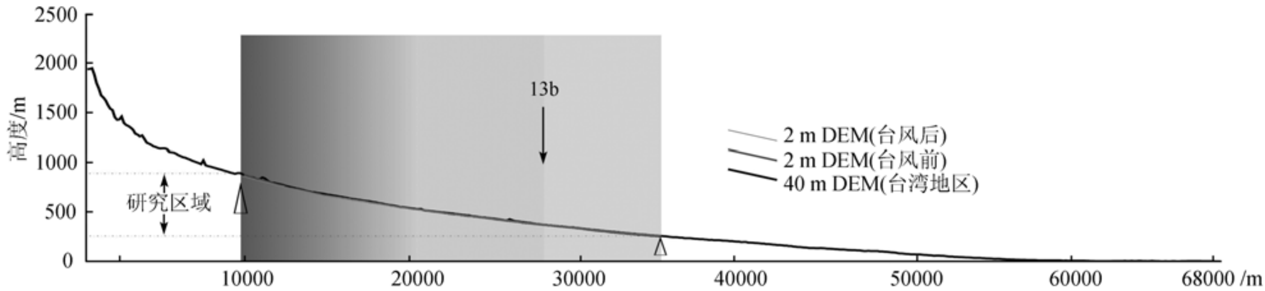

图 14 不同数值地形模型数据中的兰阳溪纵剖面

的资料作对比，以 2008 年本研究区域历经 4 次台风，范围内河道体积变化量共减少约 235 万余 m^3，依 2008 年水文数据推算研究区域范围悬移载约为 296 万余 m^3，总输沙量约为 531 万余 m^3，底床载与悬浮载比值为 9:11。若可以将河道土石体积变化量视为推移质的变化量时，以推移质与悬移质比例计算，使用过去台湾经验值 1:5 计算(郑锦桐等，2005)，悬移质体积量约为 1175 万余 m^3，沉积物总量约为 1410 万余 m^3，若使用 3:7 的比例(Dadson 等，2003)，悬移质体积量约为 548.33 万余 m^3，沉积物总量约为 783 万余 m^3，若使用 15%计算(林致远，2004)，悬移质体积量约为 1566.66 万余 m^3，沉积物总量约为 1801.66 万余 m^3。对比前人研究成果(林致远，2004；Kao 和 Liu，2001)，使用 3:7 的比例(Dadson 等，2003)较为合理接近 Kao 和 Liu(2001)的重新估算的结果，但与本研究推算的比值为 9:11 仍有差异，显示兰阳溪在暴雨时河道输沙能量显然受到低估，未来在水利工程规划上应考虑这点。

6 结 论

本研究首次应用航空激光雷达系统在大流域面积测量河道地形，并于台风季节前后不同时期的 DEM 数据，应用高程差值的地形计量方法，来计算兰阳溪在台风季节前后地形的变化，研究结果显示航空激光雷达高解析数值地形模型数据，应用在河道地形变迁以及沉积物变化量计算可以得到极佳的成果。

兰阳溪河道在 2008 年历经 4 次台风后，利用台风季节前后两次飞航任务的结果，所产生的数值地形模型数据直接计算分析，将两次飞航扫瞄测量数据，运

用两次不同时间所获取之高程资料推估地形变化量，显示在研究区域内主要仍受侵蚀影响，而搬运流失高达 230 万 m^3 土石量。

由研究区域横剖面高程差值和数据显示，图 12 中 13a 以上河道属于上游侵蚀段及中游搬运段之特性，而 13b 以下则以中游搬运段之特性。河道搬运主要控制因素应为河道坡度，河道坡度越大，侵蚀作用越明显；局部则受河道宽度及河流曲率影响，而岩性分布也影响受限河谷及河道两岸侵蚀、搬运的特性。

2008 年本研究区域内河道体积变化量共减少约 235 万余 m^3，若可以将河道土石体积变化量视为推移质的变化量时，依 2008 年水文数据推算研究区域悬移载约为 296 万余 m^3，总输沙量约为 531 万 m^3，底床载与悬浮载比值为 9 : 11，比值显示兰阳溪在暴雨时河道输沙能量被明显低估，未来在水利工程规划上应考虑此点。

参考文献(References)

Brasington J, Langham J and Rumsby B. 2003. Methodological sensitivity of morphometric estimates of coarse fluvial sediment transport. Geomorphology, 53(3–4): 299–316 [DOI: 10.1016/S0169-555X(02)00320-3]

Cavalli M, Tarolli P, Marchi L and Dalla Fontana G. 2008. The effectiveness of airborne LiDAR data in the recognition of channel-bed morphology. Catena, 73(3): 249–260 [DOI: 10.1016/j.catena.2007.11.001]

陈翰霖，张瑞津. 2007. 曾文溪流域暴大雨事件的流量及输沙量. 地理学报, (48): 43–65

Dadson S J, Hovius N, Chen H, Dade W B, Hsieh M L, Willett S D, Hu J C, Horng M J, Chen M C, Stark C P, Lague D and Lin J C. 2003. Links between erosion, runoff variability and seismicity in the Taiwan orogen. Nature, 426(6967): 648–651 [DOI: 10.1038/nature02150]

何春荪. 1986. 台湾地质概论，台湾地质图说明书. 第 2 版. 中国台湾：中国台湾地质调查所出版社: 164

Kao S J and Liu K K. 2001. Estimating the suspended sediment load by using the historical-Hydrometric record from the Lanyang-His watershed. TAO, 12(2): 401–414

Lane S N and Richards K S. 1998. High resolution, two-dimensional spatial modelling of flow processes in a multi-thread channel. Hydrological Processes, 12(8): 1279–1298 [DOI: 10.1002/(SICI)1099–1085(19980630)12:8<1279::AID-HYP615>3.0.CO;2-E]

Lane S N, Richards K S and Chandler J H. 1994. Developments in monitoring and modelling small-scale river bed topography. Earth Surface Processes and Landforms, 19(4): 349–368 [DOI: 10.1002/esp.3290190406]

Lane S N, Westaway R M and Murray Hicks D. 2003. Estimation of erosion and deposition volumes in a large, gravel-bed, braided river using synoptic remote sensing. Earth Surface Processes and Landforms, 28(3): 249–271 [DOI: 10.1002/esp.483]

林启文，林伟雄. 1995. 台湾东北部兰阳溪中下游地质构造研究.中国台湾地质调查所汇刊, 10: 23–49

林致远. 2004. 兰阳溪泥砂来源与下游河道冲淤关系之探讨. 兰阳溪生命史：宜兰研究: 113–129

Milan D J, Heritage G L and Hetherington D. 2007. Application of a 3D laser scanner in the assessment of erosion and deposition volumes and channel change in a proglacial river. Earth Surface Processes and Landforms, 32(11): 1657–1674 [DOI: 10.1002/esp.1592]

Rumsby B T, Brasington J, Langham J A, McLelland S J, Middleton R and Rollinson G. 2008. Monitoring and modelling particle and reach-scale morphological change in gravel-bed rivers. Applications and Challenges Geomorphology, 93(1-2): 40–54 [DOI: doi:10.1016/j.geomorph.2006.12.017]

Wheaton J M, Brasington J, Darby S E and Sear D A. 2010. Accounting for uncertainty in DEMs from repeat topographic surveys: improved sediment budgets. Earth Surface Processes and Landforms, 35(2): 136–156 [DOI: 10.1002/esp.1886]

吴永助. 1976. 清水土场地热区及其外围之地质. 矿业技术，14: 484–489

江阳圣，陈锟山，梁隆鑫，王志添. 2007. 以 SPOT 影像及数值地形模型推估集水区泥砂产量. 航测及遥测学刊, 12(4): 447–456

詹新甫. 1976. 台湾雪山山脉之褶皱与块体运动. 中国台湾地质调查所汇刊, 25: 29–34

郑锦桐，顾承宇，邱显晋，张玉麟，陈锦清. 2005. 遥测方法应用于集水区泥砂产量推估之研究. 中兴工程季刊, (87): 1–5

汤振辉,杨健一.1976.台湾雪山岭东北端新、古第三系间之地层缺失. 台湾石油地质, 13: 139–147

朱怡亭，徐美玲. 2007. 玉峰集水区台风事件河川流量和悬移质浓度关系之研究. 地理学报, (49): 1–22